



**HAL**  
open science

## Three novel rhamnogalacturonan I- pectins degrading enzymes from *Aspergillus aculeatinus*: Biochemical characterization and application potential

Adrien Lemaire, Catalina Duran Garzon, Aurore Perrin, Olivier Habrylo, Pauline Trezel, Solène Bassard, Valérie Lefebvre, Olivier van Wuytswinkel, Anaïs Guillaume, Corinne Pau-Roblot, et al.

### ► To cite this version:

Adrien Lemaire, Catalina Duran Garzon, Aurore Perrin, Olivier Habrylo, Pauline Trezel, et al.. Three novel rhamnogalacturonan I- pectins degrading enzymes from *Aspergillus aculeatinus*: Biochemical characterization and application potential. *Carbohydrate Polymers*, 2020, 248, pp.116752 -. 10.1016/j.carbpol.2020.116752 . hal-03492390

**HAL Id: hal-03492390**

**<https://hal.science/hal-03492390v1>**

Submitted on 22 Aug 2022

**HAL** is a multi-disciplinary open access archive for the deposit and dissemination of scientific research documents, whether they are published or not. The documents may come from teaching and research institutions in France or abroad, or from public or private research centers.

L'archive ouverte pluridisciplinaire **HAL**, est destinée au dépôt et à la diffusion de documents scientifiques de niveau recherche, publiés ou non, émanant des établissements d'enseignement et de recherche français ou étrangers, des laboratoires publics ou privés.



Distributed under a Creative Commons Attribution - NonCommercial 4.0 International License

1 **Three novel rhamnogalacturonan I- pectins degrading enzymes from**  
2 ***Aspergillus aculeatinus*: biochemical characterization and**  
3 **application potential**

4

5

6 **AUTHORS LIST**

7 Adrien Lemaire<sup>1§</sup>, Catalina Duran Garzon<sup>1§</sup>, Aurore Perrin<sup>2</sup>, Olivier Habrylo<sup>2</sup>, Pauline  
8 Trezel<sup>1</sup>, Solène Bassard<sup>1</sup>, Valérie Lefebvre<sup>1</sup>, Olivier Van Wuystwinkel<sup>1</sup>, Anaïs  
9 Guillaume<sup>2</sup>, Corinne Pau-Roblot<sup>1#</sup>, Jérôme Pelloux<sup>1#</sup>

10

11 <sup>1</sup> : UMRT INRAE 1158 BioEcoAgro – BIOPI Biologie des Plantes et Innovation, SFR  
12 Condorcet FR CNRS 3417, Université de Picardie, 33 Rue St Leu, 80039 Amiens,  
13 France. <sup>2</sup> : Centre de Recherche et Innovation Soufflet, 1 rue de la Poterne à Sel,  
14 10400 Nogent sur Seine, France.

15

16 §: These authors contributed equally to the work as first authors.

17 #: These authors contributed equally to the work as last authors.

18

19 **ABSTRACT (149 words)**

20 Rhamnogalacturonans I (RGI) pectins, which are a major component of the  
21 plant primary cell wall, can be recalcitrant to digestion by commercial enzymatic  
22 cocktails, in particular during fruit juice clarification process. To overcome these  
23 problems and get better insights into RGI degradation, three RGI degrading enzymes  
24 (RHG: Endo-rhamnogalacturonase; ABF:  $\alpha$ -Arabinofuranosidases; GAN: Endo- $\beta$ -1,4-  
25 galactanase) from *Aspergillus aculeatinus* were expressed in *Pichia pastoris*, purified  
26 and fully biochemically characterized. All three enzymes showed acidic pH optimum,  
27 and temperature optima between 40 to 50 °C. The  $K_m$  values were 0.5 mg.ml<sup>-1</sup>, 1.64  
28 mg.ml<sup>-1</sup> and 3.72 mg.ml<sup>-1</sup> for RHG, ABF, GAN, respectively. NMR analysis confirmed  
29 an endo-acting mode of action for RHG and GAN, and exo-acting mode for ABF. The  
30 application potential of these enzymes was assessed by measuring changes in  
31 viscosity of RGI-rich camelina mucilage, showing that RHG-GAN enzymes induced a  
32 decrease in viscosity by altering the structures of the RGI backbone and sidechains.

33

34 **KEY WORDS**

35 RGlases, *Aspergillus aculeatinus*, camelina mucilage, RGI-type pectins

36

37

## 38 INTRODUCTION (7701words)

39 In plants, pectin is a heteropolysaccharide mainly present in the middle  
40 lamella and primary cell wall, and is deposited during early stages of growth and cell  
41 expansion (Voragen, Coenen, Verhoef & Schols, 2009). Four pectic domains can be  
42 described: Homogalacturonan (HG), Rhamnogalacturonan type I (RGI),  
43 Rhamnogalacturonan type II (RGII) and Xylogalacturonan (XGA) (Mohnen, 2008).  
44 RGI, which is the second most abundant and complex polysaccharide in the primary  
45 cell wall (i.e. 20-35% of pectins) consists of a backbone composed of the repeating  
46 diglycosyl units ( $\rightarrow 2$ )- $\alpha$ -L-Rhap-( $1 \rightarrow 4$ )- $\alpha$ -D-GalpA-( $1 \rightarrow$ ), partly substituted, at O-4  
47 and/or O-3 positions of  $\alpha$ -L-Rhap residues, with side chains of ( $1 \rightarrow 5$ )- $\alpha$ -L-arabinans,  
48 ( $1 \rightarrow 4$ )- $\beta$ -D-galactans, arabinogalactans I (AGI), arabinogalactans-II (AG II), and  
49 possibly galactoarabinans (GAs) (Silva, Jers, Meyer & Mikkelsen 2016; Yapo, 2011).

50 To effectively degrade this complex network, one of the most important  
51 group of enzymes used in fruit and vegetable processing industry is pectinases, and  
52 in particular microbial-derived RGI-degrading enzymes (RGlases), which lowers  
53 viscosity, allows efficient mash pressing during juice clarification process and remove  
54 the mucilage coat, for instance in coffee beans. (Grassin & Fauquembergue, 1996;  
55 Tapre & Jain, 2014, Kashyap, Vohra, Chopra & Tewari, 2001). A number of RGlases  
56 have been described from *Aspergillus aculeatus*, due to its fermentation capabilities  
57 and high level of protein secretion (De Vries, Benen, de Graaff & Visser 2002; Rytioja  
58 et al., 2014). Genome sequencing among species in the *Aspergillus* genus combined  
59 to a phylogenetic and phenotypic approaches, showed that there are closely related  
60 novel species including *A. aculeatinus*, which was used in this study. It has an  
61 extensive and highly conserved set of genes encoding RGlases (Vesth et al., 2018),  
62 and therefore, considerable potential to secrete cell wall degrading enzymes.

63 The degradation of RGI backbone is realized by RGlases specific for  
64 cleaving bonds in the repetitive ( $\rightarrow 2$ )- $\alpha$ -L-Rhap-( $1 \rightarrow 4$ )- $\alpha$ -D-GalpA-( $1 \rightarrow$ ) disaccharidic  
65 units (Silva et al., 2016). Endo-rhamnogalacturonase, RHG (GH28 - EC 3.2.1.171),  
66 catalyze the hydrolysis of the  $\alpha$ -D-GalpA-( $1 \rightarrow 2$ )- $\alpha$ -L-Rhap glycosidic linkages,  
67 releasing the non-reducing end of Rhap (Suykerbuyk et al., 1997). The first  
68 discovered endo-rhamnogalacturonase enzyme was the RhgA from *A. aculeatus*,  
69 and it is one of the more extensively characterized RGI modifying enzymes (Kofod et  
70 al., 1994). Besides, accessory RGlases, which catalyze the hydrolysis of internal or

71 terminal linkages of the arabinan and galactan sidechains (Silva et al., 2016) can  
72 also be found. For example,  $\alpha$ -Arabinofuranosidase, ABF (GH54 - EC 3.2.1.55) can  
73 remove terminal non-reducing arabinose residues on arabinans and on the short side  
74 chains of arabinogalactans (Chacón-Martínez et al., 2004; de Wet, Matthew,  
75 Storbeck, van Zyl & Prior 2008; Miyanaga et al., 2006). Several  $\alpha$ -  
76 Arabinofuranosidases have been purified from *A. niger*, and only one from *A.*  
77 *aculeatus*, reporting an activity on  $\alpha$ -(1 $\rightarrow$ 2),  $\alpha$ -(1 $\rightarrow$ 3) and  $\alpha$ -(1 $\rightarrow$ 5) linked arabinose  
78 residues (Beldman, Searle-van Leeuwen, De Ruiter, Siliha, & Voragen 1993; de  
79 Vries & Visser, 2001; Saha, 2000). Among accessory RGLases, arabinogalactanases,  
80 GAN (GH53 - EC 3.2.1.89), catalyze the degradation of the galactan side chains at  $\beta$ -  
81 (1 $\rightarrow$ 4) linkages and galactanases, GAL (GH35 - EC 3.2.1.-) at  $\beta$ -(1 $\rightarrow$ 3) and  $\beta$ -(1 $\rightarrow$ 6)  
82 linkages (Le Nours et al., 2003; Silva et al., 2016). So far, the majority of  
83 arabinogalactanases from *A. aculeatus* are endo- $\beta$ -1,4-galactanase (Christgau,  
84 Sandal, Kofod, & Dalbøge, 1995; Le Nours et al., 2003; Ryttersgaard, Lo Leggio,  
85 Coutinho, Henrissat, Larsen, 2002; Torpenholt, Poulsen, Muderspach, De Maria & Lo  
86 Leggio, 2019). To assess the application potential of these enzymes, one can follow  
87 the changes in viscosity of RGI-rich pectic matrix upon their application. If pectins  
88 from fruits can be, to some extent, rich in RGI, it presents as well some HG domains  
89 which can interfere in the viscosity assay (Wefers, Flörchinger, & Bunzel, 2018;  
90 Arnous & Meyer, 2009). In contrast, seed coat mucilage appears as a substrate of  
91 interest to test the effects of the enzymes, considering its polysaccharide  
92 composition, and its use as hydrocolloid in the pharmaceutical and food industry  
93 (Ubeyitogullari and Ciftci, 2020). The seed coat mucilage composition appears highly  
94 variable, depending upon species. In *Arabidopsis* it is mainly composed of  
95 unbranched RG-I, while in *Plantago ovata* the predominant polysaccharide is  
96 arabinoxylan (Macquet, Ralet, Kronenberger, Marion-Poll, & North, 2007; Guo, Cui,  
97 Wang, & Young, 2008). *Camelina sativa*, a Brassicaceae, has received considerable  
98 interest for its potential use (Malik, Tang, Sharma, Burkitt, Ji, Mykytyshyn et al., 2018)  
99 in a large panel of applications. *Camelina* mucilage is rich in RG-I, even though its  
100 fine chemical composition remains unresolved. The rheological properties of the  
101 polysaccharide could for instance change by the presence or absence of neutral side  
102 chains.

103 The aims of this study are to 1) to produce three *A. aculeatinus* RG-I-active  
104 enzyme by recombinant expression in *Pichia pastoris* and determine their

105 biochemical properties, 2) to isolate Camelina seed coat mucilage and characterize  
106 its RG-I content and 3) to apply the enzymes (singularly and in combination) to  
107 establish their ability to modify (decrease) viscosity of Camelina RG-I mucilage. Our  
108 hypothesis is that the combined action by the recombinant *A. aculeatinus* RG-I  
109 enzymes can significantly reduce viscosity of Camelina mucilage.

110

## 111 **MATERIALS & METHODS**

### 112 **Commercial RGI substrates**

113 Pectic galactan - P-PGAPT, Arabino galactan - P-ARGAL, Arabinan - P-  
114 ARAB, debranched Arabinan - P-DBAR, azurine-cross-linked Rhamnogalacturonan I  
115 - I-AZRHI and soybean Rhamnogalacturonan - P-RHAGN substrates were  
116 purchased from Megazyme® (Bray, Co. Wicklow, Ireland).

117

### 118 ***Aspergillus aculeatinus* culture and cDNA obtention**

119 *Aspergillus aculeatinus* SCCO822 strain was kindly provided by Soufflet  
120 Research & Innovation Centre (CRIS, Nogent-sur-Seine, France). *Aspergillus*  
121 *aculeatinus* strain was cultivated in M3 medium (Mitchell, Vogel, Weimann,  
122 Pasamontes & van Loon, 1997) with different carbon sources (rich and poor RGI  
123 medium) in order to stimulate RGase expression (**Table S1**). After 14 days of culture  
124 at 27 °C, mycelium was harvested and ground in liquid nitrogen with a mortar and  
125 pestle. Total RNAs isolation was performed with RNA easy plant mini kit  
126 (Qiagen, Hilden, Germany). Freshly extracted RNAs (14 ng.µl<sup>-1</sup>) were treated with  
127 TURBO DNA-free Kit (Invitrogen, Carlsbad, California, United States) and cDNA was  
128 synthesized with Transcriptor High Fidelity cDNA Synthesis Kit (Roche, Basel,  
129 Switzerland) using anchored-oligo(dT)18 primer.

130

### 131 **Cloning and heterologous expression of RGase**

132 *A. aculeatinus* (Genome reference: NW\_020291493.1) endo-  
133 rhamnogalacturonase, RHG (GH28 - EC 3.2.1.171) (GenBank Gene ID: 37148665),  
134 endo-β-1,4-galactanase, GAN (GH53 - EC 3.2.1.89) (GenBank Gene ID: 37150470)  
135 and α-Arabinofuranosidase, ABF (GH54 - EC 3.2.1.55) (GenBank Gene ID:  
136 37152657) were amplified from *A. aculeatinus* cDNAs. Cloning primers used are  
137 listed in **Table 1**. ORFs from RHG and ABF were cloned into pPICZαB, including

138 their signal peptide, with the use of BstBI (to remove  $\alpha$ -factor from vector) and NotI  
139 restriction enzymes (New England Biolabs, Hitchin, UK). As GAN ORF contain a  
140 BstBI restriction site, it was not possible to clone it using the same procedure. GAN  
141 ORF was cloned downstream of pPICZ $\alpha$ B  $\alpha$ -factor with EcoRI and NotI restriction  
142 enzymes (New England Biolabs, Hitchin, UK). The three sequences were cloned in  
143 frame with polyhistidine tag. *Pichia pastoris* (X-33) cells were used as host cells for  
144 heterologous expression and were transformed as detailed in the EasySelect Pichia  
145 Expression Kit manual (Invitrogen, Carlsbad, California, United States).

146 **Table 1.** Primers used for cloning *Aspergillus aculeatinus* RGlases into pPICzαB  
 147 expression vectors. RHG: Endo-rhamnogalacturonase; ABF: α-  
 148 Arabinofuranosidases; GAN: Endo-β-1,4-galactanase.

Enzyme	Gene ID	Forward	Reverse
RHG	37148665	AATTTTCGAAACGATGATGCGTGCT CTTTTCCTTCTTG	TGCACGCGGCCGCGCCTGCCAAGG CACTGTAC
GAN	37150470	TCTAAGAATTACGCGCTCACCTA TCGCGG	TGCACGCGGCCGCGAGCTCCCCGA GAGTCTCGA
ABF	37152657	AATTTTCGAAACGATGATGCCTTCA CGACGAACCCTC	TGCACGCGGCCGCGCGGACGCAA AGCCC

149

## 150 **Recombinant protein expression and purification**

151 Recombinant RGlases were produced and purified by affinity  
 152 chromatography as described in Voxeur et al., 2019. Briefly, transformed *P. pastoris*  
 153 cells were grown on buffered glycerol-complex medium at 30°C in baffled flasks  
 154 before the induction step, which begins with the transfer of the cells into a medium  
 155 without glycerol but with 0.5% methanol. During 72h, the medium is kept at this  
 156 concentration by daily addition of methanol. Supernatants are recovered after  
 157 centrifugation (1 500×g, 8 min, 4 °C) and filtered with GD/X 0.45 μm PES filter Media  
 158 (Whatman, Maidstone, United Kingdom). Purification is performed by affinity  
 159 chromatography (IMAC) with a 1 ml HisTrap excel column (GE Healthcare, Chicago,  
 160 Illinois, United States). Every buffer and supernatant were kept on ice during  
 161 purification. 100 ml supernatant was loaded onto the column at a 1 ml.min<sup>-1</sup> flow rate.  
 162 HisTrap column was washed with 10 column volumes of wash buffer (25 mM  
 163 imidazole, 250 mM NaCl, 50 mM NaP pH 7,5). Target protein was recovered with 15  
 164 ml of elution buffer (250 mM imidazole, 250 mM NaCl, 50 mM NaP pH 7.5). RGlases  
 165 were concentrated with Amicon Ultra Centrifugal filter with a 10 kDa cut-off (Merck  
 166 Millipore, Burlington, Massachusetts, United States). Buffer exchange of  
 167 concentrated and purified RGlases was performed using PD Spintrap G-25 column  
 168 (GE Healthcare).

169

## 170 **Protein Electrophoresis**

171 Protein concentrations were determined by the Pierce BCA Protein Assay Kit  
 172 (Thermo Fisher Scientific, Waltham, Massachusetts, United States) with Bovine  
 173 Serum Albumin (A7906, Sigma) as standard. Molecular weight and homogeneity



174 were estimated by polyacrylamide gel electrophoresis under denaturing conditions  
175 using mini-PROTEAN 3 system (BioRad, Hercules, California, United States).  
176 Proteins were revealed using PageBlue Protein Staining Solution (Thermo Fisher  
177 Scientific) according to the manufacturer's protocol. Deglycosylation of RGases were  
178 performed using Peptide-N-Glycosidase F (PNGase F) at 37 °C for one hour  
179 according to the supplier's protocol (New England Biolabs, Hitchin, UK).

180

### 181 **Microplate assay**

182 The activities of the endo- $\beta$ -1,4-galactanase (GAN),  $\alpha$ -arabinofuranosidase  
183 (ABF) and endo-rhamnogalacturonase (RHG) enzymes were determined using the  
184 DNS method (Miller, 1959). The reaction consisted of 0.5 % (w/v) pectic galactan or  
185 arabinogalactan diluted in 50 mM sodium acetate (pH 4.5) for GAN; 0.5 % (w/v)  
186 arabinan or debranched arabinan diluted in 50 mM McIlvaine buffer (McIlvaine, 1921)  
187 (pH 4.0) for ABF and 0.5 % (w/v) rhamnogalacturonan diluted in sodium acetate  
188 buffer (pH 4.5) for RHG. Three  $\mu$ g of enzyme in 25  $\mu$ L final volume was incubated at  
189 40 °C for 15 min for all reactions. The reactions were stopped with 150  $\mu$ L of DNS  
190 reagent, boiled at 95 °C for 8 min and cooled down for color stabilization. The  
191 absorbance was measured at 540 nm using Powerwave XS2 (BioTek Instruments,  
192 Inc, VT, USA) equipment. L-(+)-Arabinose and D-(+)-Galactose were used as  
193 standards for ABF and GAN, activity tests, respectively. The recombinant RHG  
194 activity was also assayed with 0.5 % (w/v) azurine-cross-linked  
195 Rhamnogalacturonan-I (AZCL-RGI) at 40 °C for 15 min in 100  $\mu$ L of 50 mM sodium  
196 acetate buffer (pH 4.5). The reaction was terminated by adding 100  $\mu$ L of 10 % Tris  
197 pH 10 and measured at 595 nm. A calibration curve of AZCL-RGI was made by 3 h-  
198 incubation with concentrated RHG at optimal activity. All experiments were  
199 conducted in triplicates with a blank sample and the increase in the absorbance was  
200 proportional to the amount of substrate released in all assays.

201

### 202 **Effects of pH and temperature**

203 The optimum pH was determined between pH 3 and 8 using 50 mM citrate  
204 acid buffer (pH 3 to 3.5), sodium acetate buffer (pH 3.5 to 5) and McIlvaine buffer (pH  
205 5 to 8) and pectic galactan for GAN, AZCL-RGI for RHG and arabinan for ABF, at  
206 40°C. The pH stability was assessed by incubating the enzymes at pHs values from  
207 3 to 8, at 40 °C for 90 min, using 50 mM of the above-mentioned buffer solutions. To

208 determine the optimum temperature, enzymatic reactions were performed between  
209 30°C and 70°C in 50 mM sodium acetate buffer pH 4.5 with pectic galactan for GAN,  
210 AZCL-RGI for RHG, and 50 mM McIlvaine buffer pH 4.0 with arabinan for ABF.  
211 Temperature stability was determined by measuring the residual activity after 30 min  
212 of preincubation of the enzyme at temperatures between 30 °C and 70 °C in 50 mM  
213 sodium acetate buffer, pH 4.5 and McIlvaine buffer pH 4.0. For the pH stability the  
214 residual enzyme activity was assayed using 0.5 % (w/v) pectic galactan for GAN,  
215 AZCL-RGI for RHG and arabinan for ABF as substrate in the optimal condition for  
216 each enzyme after 90 min preincubation at given pH between 3 and 8 at 30°C.

217

### 218 **Determination of Km, Vmax, and specific activity**

219 The kinetic parameters Vmax and Km were calculated by GraFit7 software  
220 (Michaelis-Menten/Hill; Erithacus Software, Horley, Surrey, UK), using pectic  
221 galactan for GAN, AZCL-RGI for RHG and arabinan for ABF. The reactions were  
222 performed at the optimum pH and temperature, using 0.05 to 4 g.mL<sup>-1</sup> substrate  
223 concentrations.

224

### 225 **Mucilage extraction and hydrolysis**

226 Seeds from *Camelina sativa* for mucilage extraction were kindly provided by  
227 Biogis Center (SAS PIVERT, Compiègne, France). Mucilage from *Camelina sativa*  
228 was extracted following an adapted protocol (Sarv et al., 2017). It consists of 1h  
229 water imbibition of seeds at room temperature under slow stirring followed by  
230 filtration, ethanol precipitation and freeze-drying. For monosaccharides composition  
231 determination, 1 mg of freeze-dried mucilage was treated during 2 h at 120 °C with 1  
232 ml.mg<sup>-1</sup> of 4 M trifluoroacetic acid to maximize monosaccharide recovery.  
233 Monosaccharides were dried under a nitrogen stream and resuspended in 1 ml of  
234 H<sub>2</sub>O. Samples were filtered through a 13 mm 0.2 µm nylon econofilter (Agilent  
235 technologies) before HPAEC analysis.

236

### 237 **Monosaccharide composition determination**

238 The cell wall monosaccharide composition was determined by high-  
239 performance anion-exchange chromatography (HPAEC) with a pulsed amperometric  
240 detector (Dionex ICS 3000 system). After hydrolysis of mucilage, aliquots of the  
241 extract were injected through a 4x50 mm CarboPac PA1 pre-column (Dionex) before

242 separation of anionic compounds on a 4x250 mm CarboPac PA1 column (Dionex) at  
243 30 °C. For neutral and acid monosaccharides, a multi-step gradient analyse was  
244 used as in Pillon et al., 2010. Peak analysis was performed using Chromeleon  
245 software, version 7.0. Standard of fucose, arabinose, rhamnase, glucose, galactose,  
246 xylose, mannose, galacturonic acid and glucuronic acid from  $5.0 \times 10^{-4}$  to  $2.5 \times 10^{-1}$   
247 mg.ml<sup>-1</sup> concentration were used for quantification (Bertin et al., 2013).

248

### 249 **NMR Spectra analysis**

250 Before NMR analysis, samples were rinsed twice with 99.9 % D<sub>2</sub>O (Euriso-  
251 top), dried under vacuum, and 1 mg dissolved in 99.96% D<sub>2</sub>O (0.5 ml<sup>-1</sup>). <sup>1</sup>H NMR  
252 spectra were recorded, at room temperature on a Bruker Avance 500 spectrometer  
253 equipped with a 5 mm BBI probe and Topspin 3.1 software. <sup>1</sup>H NMR spectra were  
254 accumulated using a 30° pulse angle, a recycling time of 1 s and an acquisition time  
255 of 2 s for a spectral width of 3 000 Hz for 32 K data points with or without a  
256 presaturation of the HOD signal using a presaturation sequence provided by Bruker.  
257 The 2D <sup>1</sup>H/<sup>1</sup>H COSY, <sup>1</sup>H/<sup>1</sup>H TOCSY, <sup>1</sup>H/<sup>1</sup>H NOESY, <sup>1</sup>H/<sup>13</sup>C HSQC and <sup>1</sup>H/<sup>13</sup>C HMBC  
258 spectra were acquired with a standard pulse sequence delivered by Bruker (Bertin et  
259 al., 2015).

260

### 261 **Viscosity analysis**

262 The influence of RGlases on camelina mucilage viscosity was measured  
263 using a sino-wave Vibro viscometer (A&D Company). Two µg of the enzyme were  
264 incubated in a 13 ml water solution of camelina mucilage 4 g.l<sup>-1</sup> at 30°C pH 5.  
265 Measurements were taken at 0 min, 1 h, 2 h, and 4 h. A quarter of two µg of each  
266 enzyme (0.5 µg) was added in combination assays to allow the enzyme-effect to be  
267 discriminated and avoid dependent-dose effect. Measures were taken at 0 min, 30  
268 min, 1 h, 2 h, and 4 h.

269

### 270 **Size-Exclusion Chromatograph analysis**

271

272 SEC analysis was conducted using a GPCmax/Viscotek TDA305 (Malvern) equipped  
273 with quadruple detection. Columns used for the SEC separation were a Malvern  
274 A5000 and a A6000M (Malvern) connected in series, calibrated on PEO 24K and  
275 verified with Dextran T73K.

276 All the analyses were carried out using NaNO<sub>3</sub> 50mM + 0.02% sodium azide as  
277 eluent. Detectors were temperature regulated at 30 °C. After viscosity assays, 500 µL  
278 of all samples were diluted to 1/2 in water and inactivated by a bath at 95 °C for 10  
279 minutes. After filtration on 0.45 µl syringe filter, 100 µl was injected with a flow-rate of  
280 0.7 mL min<sup>-1</sup>.

281

## 282 **Statistical analysis**

283           Analyses were performed with R software (<http://www.R-project.org/>).  
284 Statistical comparisons among groups were carried out with one-way ANOVA and  
285 Tukey HSD multiple comparisons, p < 0.05 was considered statistically significant.  
286 Data were expressed as means ± SD.

287

288

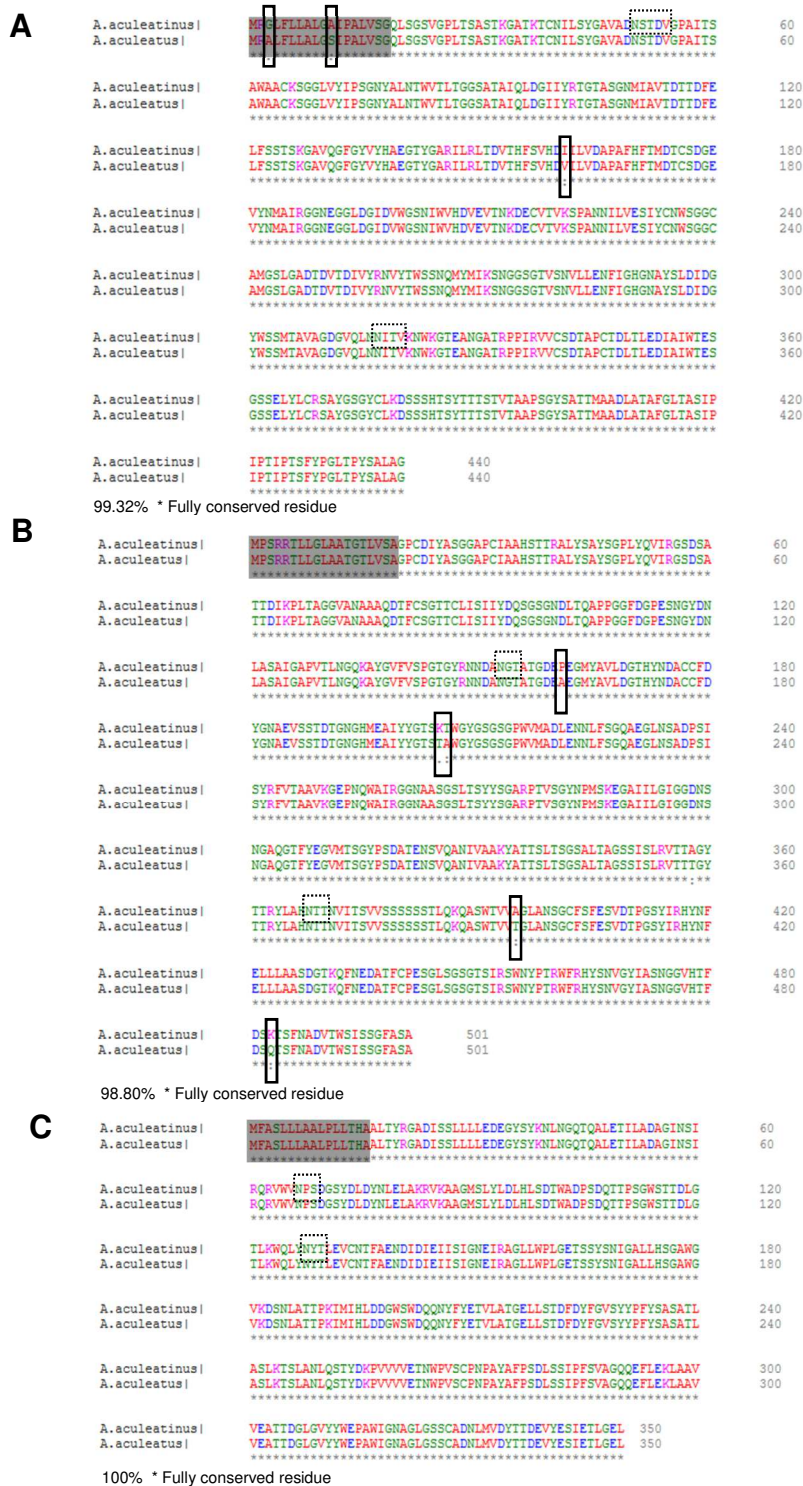
289

## 290 RESULTS AND DISCUSSION

291

### 292 ***Cloning and expression of recombinant RGlases***

293 The full-length genomic DNA sequences of endo-rhamnogalacturonase  
294 (RHG) (GenBank Gene ID: 37148665),  $\alpha$ -Arabinofuranosidases (ABF) (GenBank  
295 Gene ID: 37152657) and endo- $\beta$ -1,4-galactanase (GAN) (GenBank Gene ID:  
296 37150470) consisted of 1517 (3 introns), 1754 (no introns) and 1597 (1 intron) base  
297 pairs, respectively. RHG and GAN were amplified from cDNA from *A. aculeatinus*  
298 culture grown on soy bean RG as the expression of the genes was induced on this  
299 substrate (**Table S1**). As ABF gene does not have intron, its amplification was  
300 directly performed on genomic DNA. At the amino-acid level, the sequences were  
301 aligned as shown in **Fig. 1**. The deduced amino acid sequence showed high  
302 similarities with enzymes previously annotated from *A. aculeatus*, 99.32 % for RHG  
303 (**Fig. 1A**), 98.80 % for ABF (**Fig. 1B**) and 100 % for GAN (**Fig. 1C**). Thus, most of  
304 changed residues are conservative mutations. In addition, the structure-based  
305 sequence model revealed conserved RGlases active sites between *A. aculeatus* and  
306 *A. aculeatinus* (data not shown).



307

308

309

310

311

312

313

**Fig. 1.** Multiple alignment of amino acid sequences from *A. aculeatinus* and *A. aculeatus* for the three RGlases. The alignments were performed using ClustalW. Sequences used were as follow: (A) RHG (*A. aculeatinus*, XM\_025645590.1, NCBI REFSEQ; *A. aculeatus*, Q00001.1, Uniprot); (B) ABF (*A. aculeatinus*, XP\_025505686.1, NCBI REFSEQ; *A. aculeatus*, XP\_020052596, NCBI REFSEQ); (C) GAN (*A. aculeatinus*, XP\_025504038.1, NCBI REFSEQ; *A. aculeatus*, 1FHL\_A, PDB). Potential N-glycosylation sites are dotted-box and potential residues changes are black-boxed. Signal peptide are

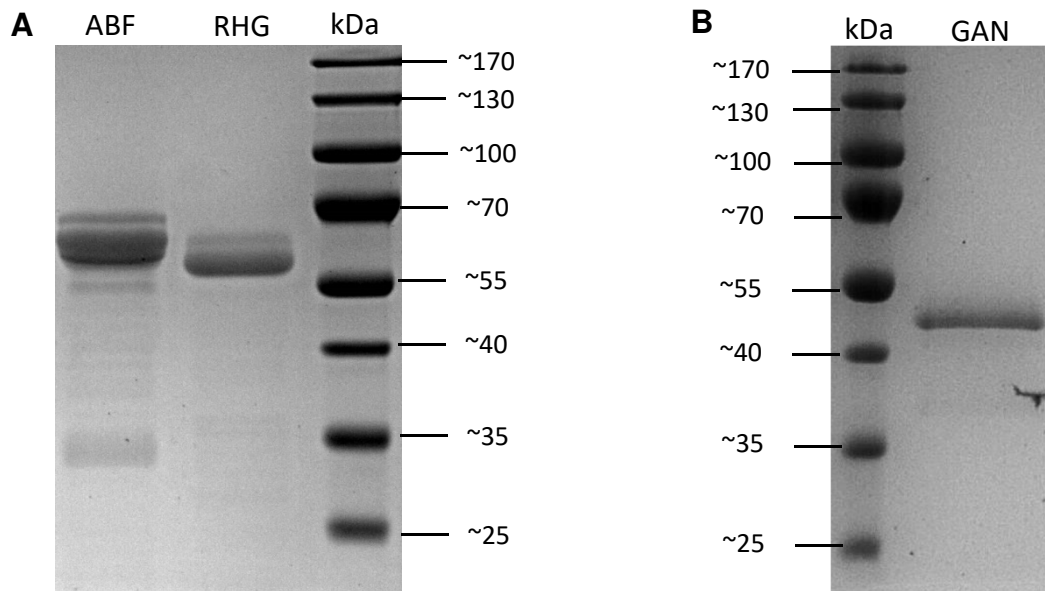
314 highlighted in grey. RHG: Endo-rhamnogalacturonase; ABF:  $\alpha$ -Arabinofuranosidases; GAN: Endo- $\beta$ -  
315 1,4-galactanase.

316

### 317 **Purification of recombinant RGlases**

318 The three enzymes were successfully produced and purified with high purity  
319 (**Fig. 2A-B**). The purified recombinant enzymes have a slightly higher apparent  
320 molecular weight compared to the predicted protein from *A. aculeatinus* (**Fig. 2. and**  
321 **Table 2**). RHG and ABF were secreted at ~66 kDa and GAN was secreted at ~50  
322 kDa, while theoretical sizes were ~48 kDa for RHG, ~53 kDa for ABF and ~40 kDa  
323 for GAN, suggesting the presence of N- or O-Glycosylation sites. Two putative N-  
324 glycosylation sites were indeed identified for RHG (32 Asn, Ser, Thr, Asp and 299  
325 Asn, Ile, Thr, Val), ABF (134 Asn, Gly, Thr, Ala and 349 Asn, Thr, Thr, Asn) and GAN  
326 (55 Asn, Pro, Ser, Asp and 116 Asn, Thr, Thr, Leu). However, the first potential site  
327 of N-glycosylation on GAN, could be hindered by the presence of Pro just after the  
328 Asn. None O-glycosylation sites were identified for the three enzymes by NetO-Glyc  
329 Server analysis. After treatment by a peptide -N-Glycosidase enzyme (PNGase F), a  
330 slight decrease in molecular mass of the proteins was observed, confirming the  
331 presence of N-glycosylation on the three enzymes (**Fig. S1**). It has been previously  
332 reported that heterologous proteins that are expressed by *P. pastoris* yeast can be  
333 glycosylated on the Asn, Ser or Thr hydroxy groups with N-linked and O-linked  
334 saccharides (usually 8–14 mannose residues) (Bretthauer & Castellino, 1999;  
335 Habrylo, Evangelista, Castilho, Pelloux & Henrique-Silva, 2018). Two potential N-  
336 glycosylation sites and discrepancies in molecular weight have been reported for  
337 RHG and GAN from *A. aculeatus* (Christgau et al., 1995; Kofod et al., 1994). In  
338 contrast, no carbohydrate was shown to be bound at the potential N-glycosylation  
339 sites in the crystallographic structure of *A. aculeatus* GAN (Ryttersgaard et al., 2002).  
340 The molecular weight obtained for the recombinant RHG is comparable to rRGase A  
341 from *A. aculeatinus* (~62Kda) with a significant amount of glycan structures attached  
342 to the enzyme reported by Kofod et al., 1994. While no reports have been found in  
343 literature for ABF from *A. aculeatus*, ABF from *A. niger* has a 64/67 kDa molecular  
344 weight and the presence of two N-linked glycosylation sites (Crous, Pretorius & van  
345 Zyl, 1996; Flipphi, van Heuvel, van der Veen, Visser, & de Graaff, 1993). In addition,  
346 literature shows that native and recombinant enzymes expressed in *P. pastoris* have  
347 similar biochemical properties, and when the N-linked glycans are not close to the

348 active site tunnel loops (as for the three characterized RGlases, **Fig. S2**), there is no  
349 impact on thermal stability and enzymatic activities (Koseki et al., 2006., Adney et al.,  
350 2009).  
351



352  
353 **Fig. 2.** SDS-PAGE of purified recombinant *A. aculeatinus* RGlases. (A) *Line 1* purified  $\alpha$ -  
354 Arabinofuranosidases (ABF); *Line 2* purified endo-rhamnogalacturonase (RHG). *Lane 3* molecular  
355 weight marker. (B) *Lane 1* molecular weight marker; *Line 2* purified endo- $\beta$ -1,4-galactanase. (GAN).  
356 Each line of purified protein contains  $\sim 3 \mu\text{g}$ . Purified proteins were resolved on a 12% acrylamide gel  
357 and stained with Coomassie brilliant blue.



358 **Table 2.** Biochemical characteristics of the purified recombinant *A. aculeatinus* RGlases. RHG: Endo-  
 359 rhamnogalacturonase; ABF:  $\alpha$ -Arabinofuranosidases; GAN: Endo- $\beta$ -1,4-galactanase.

Characteristics	RHG	ABF	GAN
Classification	GH28 - EC 3.2.1.171	GH54 - EC 3.2.1.55	GH53 - EC 3.2.1.89
MW * (kDa)	47.3	53.0	40.2
pI *	5.05	5.18	4.54
pH optimum	4.5	3.5 - 4.5	3.5 - 4.0
pH stability	5.5 - 8	3 - 8	3.5 - 6
Temperature optimum (°C)	50	40	50
Temperature stability (°C)	< 60	< 50	< 40
Km (mg/ml)	0.50 $\pm$ 0.19	1.64 $\pm$ 0.17	3.72 $\pm$ 0.59
Vmax (mg/min)	1.59 $\pm$ 0.37	1.14 $\pm$ 0.05	4.02 $\pm$ 0.39
Vmax/Km	3.18 $\pm$ 0.56	0.71 $\pm$ 0.21	1.08 $\pm$ 0.10

\* Theoretical value

360

### 361 **Biochemical characterization of recombinant RGlases**

362 The optimal activity conditions and the specificity for commercial substrate  
 363 were determined for each RGlases (**Fig. 3, Fig. 4 and Table 2**). The optimum  
 364 temperature for RHG was 50 °C (**Fig. 3A and Table 2**), remaining stable up to 40 °C  
 365 and losing 30 % of its activity at 50 °C. The effects of pH on enzyme activities  
 366 reported that RHG has maximal activity at pH 4.5 (**Fig. 3B and Table 2**). Although,  
 367 RHG was less stable at lower acidic pHs, losing 50 % of its activity for pH 3 to 5.  
 368 However, its activity remained stable (80 % activity) from pH 5.5 to 7. The  
 369 biochemical properties are conserved within their GH 28 family. Hence, our results  
 370 were strikingly different from those previously reported, (Kofod et al., 1994). This  
 371 could be related to different substrates used for the assays as the use of AZCL-RGI  
 372 to test Rhamnogalacturonan hydrolase and lyase activities was only reported from  
 373 the 2000s onwards (De Fine Licht, Schiøtt, Mueller, & Boomsma, 2010). RHG  
 374 showed the highest activity for AZCL-RGI substrate (**Fig. 4A**). In contrast, when  
 375 using rhamnogalacturonan (RG) and camelina mucilage, RHG activity was  
 376 dramatically reduced, and close to null. The RHG activity was also evaluated by <sup>1</sup>H

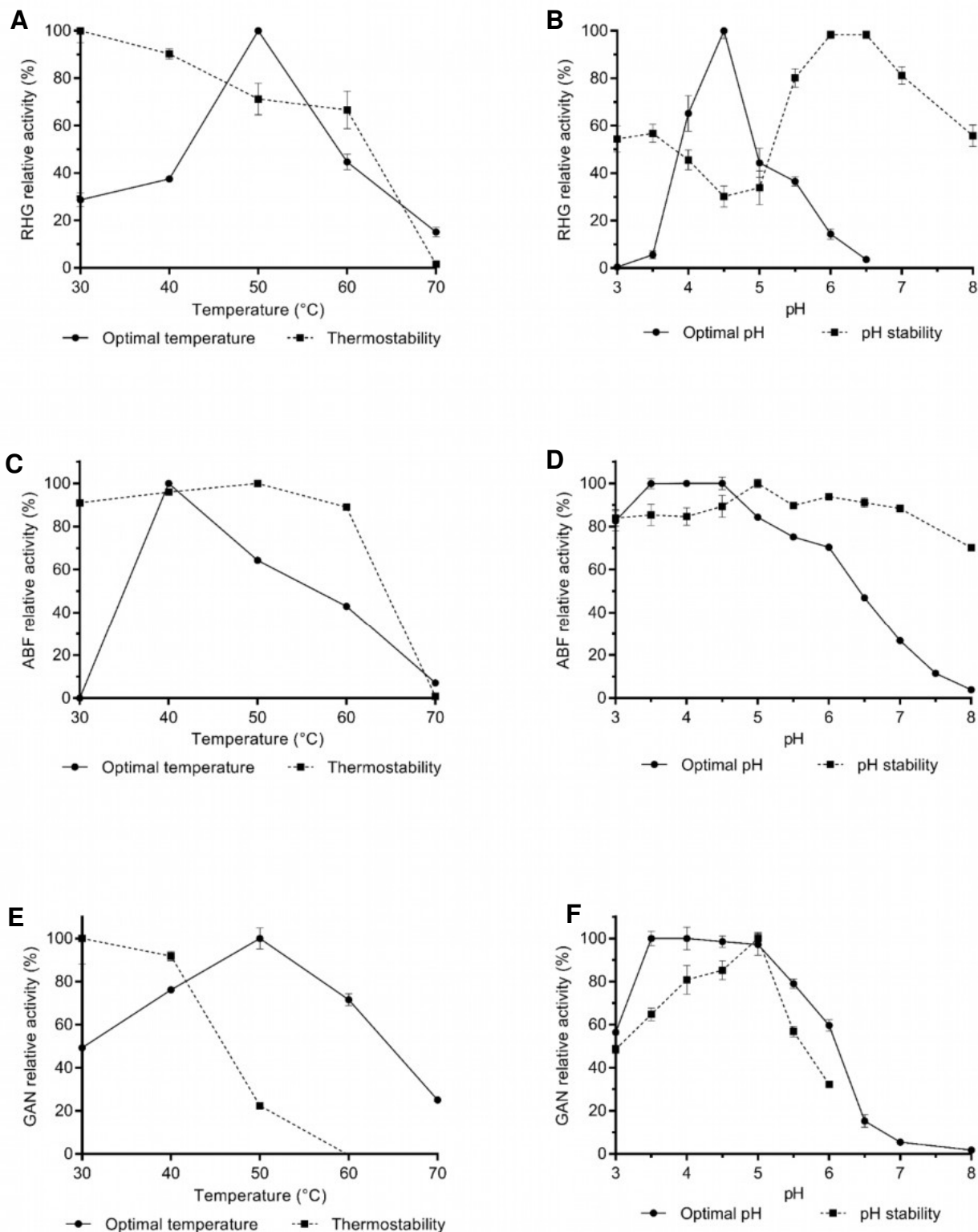
377 NMR (**Fig. 4B-C**). Due to the non-solubility of AZCL-RGI in an aqueous solvent, no  
378 signal was observed on the control spectrum (**Fig. 4B**). In contrast, the characteristic  
379 signals of RGI appeared during the hydrolysis of the chromophore part showing the  
380 activity of the RHG. The activity of RHG on RG was also assessed by <sup>1</sup>H NMR (**Fig.**  
381 **4C**): Signals observed in the spectrum at 5.24 ppm (H-1 →2)-α-Rha-(1→), 5.02 ppm  
382 (H-1 →4)-α-GalA-(1→) and 4.63 ppm (H-1 →4)-β-Gal-(1→) (Mikshina et al., 2015b;  
383 Zheng & Mort, 2008), were characteristic of the hydrolysis of the backbone of RG by  
384 an endo-RHG as no signals from rhamnose or galacturonic acid monosaccharides  
385 were detected.

386 For ABF if the optimum temperature was 40 °C (**Fig. 3C and Table 2**), the  
387 activity remained stable up to 60 °C and was inactivated at 70 °C. ABF had an  
388 optimum activity between pH 3.5 to 4.5 (**Fig. 3D and Table 2**). The ABF enzyme  
389 showed a stable activity from pH 3 to pH 7, for which more than 80 % of the activity  
390 was maintained. The ABF results are in concordance to those previously reported for  
391 ABF-GH54 family enzymes: a pH optimum between 3.5 and 5, and a temperature  
392 optimum between 50 and 60 °C (de Wet et al., 2008). ABF showed 100 % of activity  
393 for arabinan (ARAB), 20 % for debranched arabinan (D-ARAB), and very low activity  
394 was detected for camelina mucilage (MUC) (**Fig. 4D**). The activity of ABF was also  
395 studied by <sup>1</sup>H NMR. (**Fig. 4E-F**). In the spectra related to the activity of ABF on  
396 arabinan (**Fig. 4E**), the hydrolysis of the sidechains was observed by the losses of  
397 5.13 ppm (H-1 →3,5)-α-Ara-(1→) and 5.16 ppm (H-1 →3)-α-Ara-(1→) signals, as  
398 well as the appearance of the two signals of arabinose at 5.24 ppm (α-Ara) and 4.51  
399 ppm (β-Ara) (Ding, 2015; Shinozaki, Kawakami, Hosokawa & Sakamoto, 2014).  
400 These results indicated that the ABF is an exo-enzyme. ABF was also active on  
401 debranched arabinan (**Fig. 4F**) albeit to a lower extent compared to arabinan. ABF  
402 acted preferentially on →3)-α-Ara-(1→ compared to →5)-α-Ara-(1→.

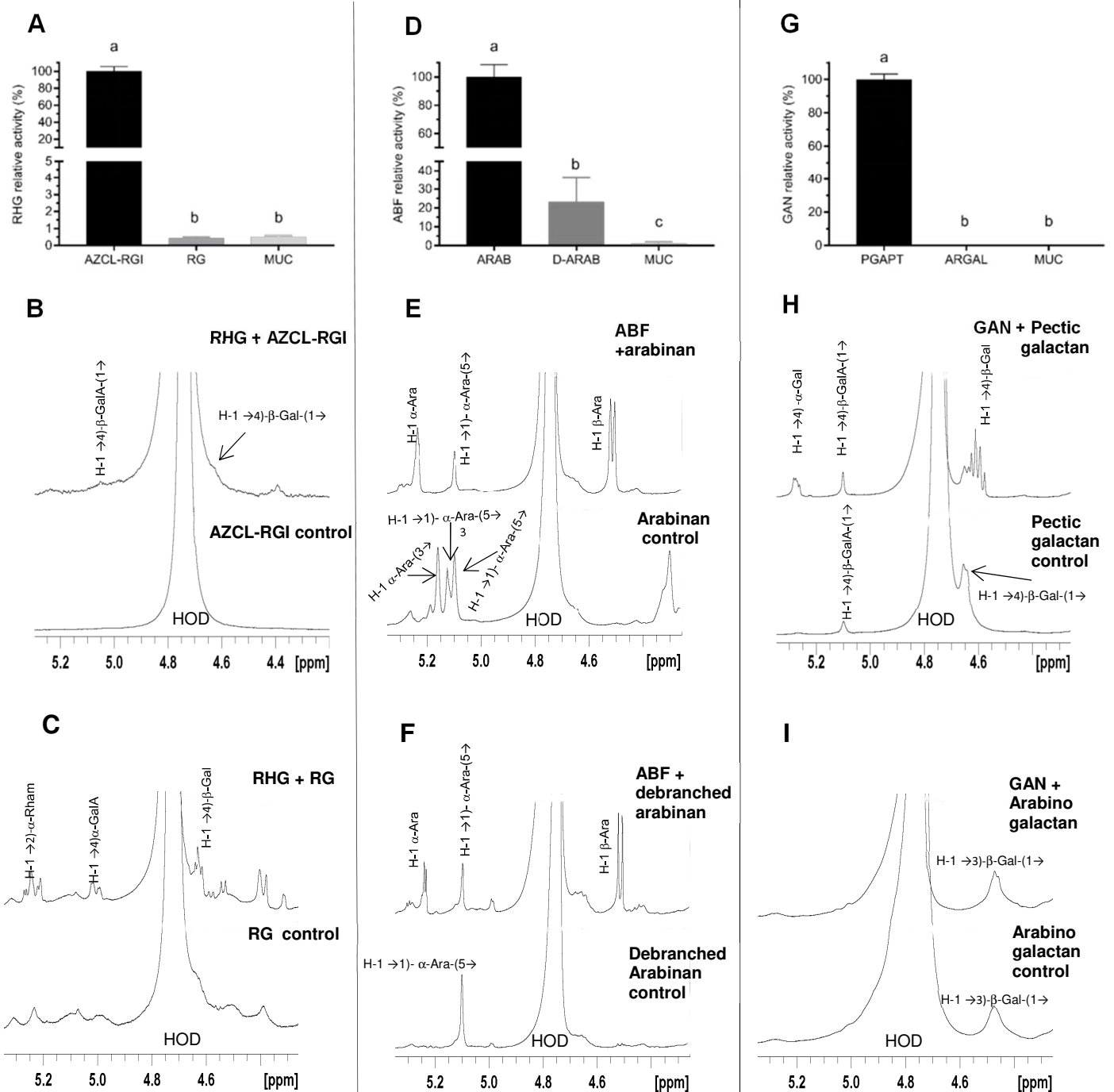
403 GAN activity showed an optimum temperature of 50 °C (**Fig. 3E and Table**  
404 **2**), although its activity decreased by 80% after a 30min incubation at 50°C and was  
405 completely inactivated above 60°C. GAN enzyme had an optimum activity for pH 3.5  
406 to 4.5 (**Fig. 3F and Table 2**). Despite its stability in the pH 4.5 to pH 5.5 range, it lost  
407 20% of its activity at pH 4 and 60 % at pH 6. GH53 enzymes – GAN have a pH  
408 optimum between 4 and 4.5 and temperature optima between 45 and 65 °C  
409 (Christgau et al., 1995; Le Nours et al., 2003). For the substrate specificity, GAN  
410 showed significant activity on galactan, while no activity was detected on

411 arabinogalactan and MUC substrates (**Fig. 4G**). NMR spectra for GAN on galactan  
412 showed the presence of signals at 4.61 ppm (H-1  $\beta$ -Gal) and 5.28 ppm (H-1  $\alpha$ -Gal)  
413 characteristics of galactoses linked in position 4 (**Fig. 4H-I**). As no signal for  
414 galactose monosaccharide was detected, we can conclude that GAN is an endo-  
415 enzyme (Cruz et al., 2010; González-Ayón et al., 2019). Moreover, based on the  $^1\text{H}$   
416 NMR spectra, and consistent with the colorimetric assay, no GAN activity was  
417 detected on arabinogalactan. As this substrate is in part constituted by  $\rightarrow 3$ )- $\beta$ -Gal-  
418 (1 $\rightarrow$ , we can conclude that GAN is specific for  $\rightarrow 4$ )- $\beta$ -Gal-(1 $\rightarrow$ .

419 Most of these results are in accordance with the reports for RHG and GAN  
420 proteins from *A. aculeatus* (Christgau et al., 1995; and Kofod et al., 1994), showing  
421 an endo-acting activity on RGI backbone and galactan, respectively. Also, the  
422 present study for *A. aculeatinus* ABF is in agreement with the ABF from *A. niger*  
423 which had action on arabinan (Flipphi et al., 1993). The kinetics parameters reported  
424 for the three RGlases characterized in our study (**Table 2**) are not easily comparable  
425 between species as substrates, pH and temperature used in the assays varied. For  
426 example,  $K_m$  values reported for GAN from *A. aculeatus*, tested with potato  
427 arabinogalactan were 10-fold lower than what we report in the present study (Van de  
428 Vis, Searle-van Leeuwen, Siliha, Kormelink, & Voragen., 1991). To our knowledge,  
429 no values have been established for RHG and ABF from *A. aculeatus*, making  
430 comparisons difficult with our present study.



431 **Fig. 3.** pH and temperature optimum for *A. aculeatinus* recombinant RGLases. (A) Influence of  
 432 temperature on RHG activity; (B) Influence of pH on RHG activity; (C) Influence of temperature on  
 433 ABF activity; (D) Influence of pH on ABF activity; (E) Influence of temperature on GAN activity; (F)  
 434 Influence of pH on GAN activity. The values are mean  $\pm$  SD for three replicates. RHG: Endo-  
 435 rhamnolacturonase; ABF:  $\alpha$ -Arabinofuranosidases; GAN: Endo- $\beta$ -1,4-galactanase.



437

438 **Fig. 4.** Substrate specificity of *A. aculeatinus* recombinant RGases. (A) RHG relative activity on AZCL-  
 439 RGI: Azurine-cross-linked rhamnogalacturonan I, RG: Rhamnogalacturonan and MUC: Camelina  
 440 mucilage. (B)  $^1\text{H}$  proton NMR spectra of RHG activity on AZCL-RGI and (C) RG. (D) ABF relative activity  
 441 on ARAB: Arabinan, D-ARAB: Debranched arabinan and MUC. (E)  $^1\text{H}$  proton NMR spectra of ABF  
 442 activity on Arabinan and on (F) Debranched arabinan. (G) GAN relative activity on PGAPT: Pectic  
 443 galactan, ARGAL: Arabino galactan and MUC. (H)  $^1\text{H}$  proton NMR spectra of GAN activity on Pectic  
 444 galactan and (I) Arabino galactan. The values of the relative activity are mean  $\pm$  SD for three replicates.  
 445 RHG: Endo-rhamnogalacturonase; ABF:  $\alpha$ -Arabinofuranosidases; GAN: Endo- $\beta$ -1,4-galactanase.

446 **Polysaccharide content of *Camelina sativa* mucilage**

447 To further evaluate the RGI enrichment in *Camelina sativa* mucilage and  
 448 describe the activity of RGlases recombinant enzymes, the monosaccharides content  
 449 of MUC was determined (**Table 3**). A 1 h stirring of the seeds in water allowed  
 450 obtention of 1.15 g of freeze-dried mucilage per 100 g of camelina seeds. To  
 451 determine sugar composition, freeze-dried mucilage was treated during 2 h at 120 °C  
 452 with 1 ml.mg<sup>-1</sup> TFA to maximize monosaccharide recovery. The HPAEC analysis  
 453 showed that *Camelina sativa* mucilage was rich in galacturonic acid, galactose and  
 454 rhamnose (~30 mol %) while minor amounts of arabinose, glucuronic acid (~5 mol  
 455 %), glucose (~3 mol %), xylose and fucose (>~1 mol %) were detected, (**Table 3**).

456  
 457 **Table 3.** Monosaccharide composition of Camelina mucilage. The values are mean ± SD for three  
 458 replicates.

Monosaccharide	Relative content (mol %)
L-Fucose	0.16 ± 0.01
L-Rhamnose	27.15 ± 1.04
L-Arabinose	5.54 ± 0.06
D-Galactose	29.55 ± 1.89
D-Glucose	2.77 ± 0.33
D-Glucuronic acid	4.11 ± 0.05
D-Galacturonic acid	30.42 ± 2.87
D-Xylose	0.30 ± 0.02

459  
 460 These values are similar to that reported by North, Berger, Saez-Aguayo, &  
 461 Ralet, 2014. The higher galacturonic acid, rhamnose and galactose contents indicate  
 462 a substrate rich in RGI, which may be highly substituted by short side-chains of  
 463 galactose and, to a lesser extent, by arabinose side-chains at Rhap O (2) and O (3)  
 464 atoms. In contrast in most cell walls, RGI are present as long side-chains of  
 465 galactans and arabinans attached to Rhap at the O(4) position (Mikshina, Petrova &  
 466 Gorshkova., 2015a). The NMR signals from MUC were identified by 2D NMR  
 467 and chemical shifts were reported in **Table 4**. The glycosidics linkages were further

468 determined by 2D NMR and selected region of the 2D NMR COSY, HSQC and  
469 NOESY spectra are reported in **Fig. S3**. The cross-peaks observed on NOESY  
470 spectrum: H-1 of  $\alpha$ -Rhap residues at 5.23 ppm with H-4 of  $\alpha$ -GalAp at 4.42 ppm and  
471 H-1 of  $\alpha$ -GalAp at 5.02 ppm with H-2 of  $\alpha$ -Rhap at 4.13 ppm indicate the presence of  
472 RG-I backbone. Cross peaks were also observed between H-1 of  $\beta$ -Galp at 4.62 ppm  
473 with H-4 of  $\alpha$ -Rhap at 3.68 ppm indicating the presence of side chain mainly  
474 composed of galactose. Very small intensity cross-peaks were also observed  
475 between H-1 of Araf (5.11 ppm) and H-3 of  $\beta$ -Galp (3.73 ppm) corroborating a partial  
476 substitution of galactose side chains by arabinose. The sugar composition allowed  
477 estimating that one side chain of galactose out of five was substituted by arabinose.  
478 The signal intensity of methyl group protons at 1.23 ppm and 1.30 ppm allowed  
479 estimating the proportion of non-branched rhamnose (53 %) and branched rhamnose  
480 (47 %) residues, respectively (Mikshina et al., 2015).

481 This result was compared with the average length of the galactose chains that were  
482 approximately 2 monomers (evaluated by the ratios of galactose and rhamnose in the  
483 polymer). These results confirmed that RGI backbone is highly substituted by short  
484 side chains of galactose which led us to propose structure of camelina mucilage:

485 Backbone :

486  $\rightarrow 2$ )- $\alpha$ -L-Rhap-(1 $\rightarrow$ 4)- $\alpha$ -D-GalAp-(1 $\rightarrow$ 2)- $\alpha$ -L-Rhap-(1 $\rightarrow$ 4)- $\alpha$ -D-GalAp-(1 $\rightarrow$

487 Main side chain:

488  $\beta$ -D-Galp-(1 $\rightarrow$ 4)- $\beta$ -D-Galp-(1 $\rightarrow$  substituted partially by  $\alpha$ -L-Araf-(1 $\rightarrow$ 3)

489 **Table 4.** Chemical shifts of <sup>13</sup>C and <sup>1</sup>H (*italics*) in ppm of the main carbohydrate sugars residues from  
 490 camelina mucilage (in D<sub>2</sub>O at room temperature). Not-determined (nd)

491	<b>Residue</b>	<b>C-1</b>	<b>C-2</b>	<b>C-3</b>	<b>C-4</b>	<b>C-5</b>	<b>C-6</b>
492		<i>H-1</i>	<i>H-2</i>	<i>H-3</i>	<i>H-4</i>	<i>H-5</i>	<i>H-6</i>
493	→4)-α-GalA-(1→	99.5 <i>5.02</i>	69.8 <i>3.90</i>	70.6 <i>4.08</i>	78.9 <i>4.42</i>	72.5 <i>4.90</i>	175.0
494	→2)-α-Rha-(1→	100.2 <i>5.23</i>	78.1 <i>4.10</i>	70.2 <i>3.88</i>	74.0 <i>3.39</i>	70.8 <i>3.77</i>	18.5 <i>1.23</i>
495							
496	→2,4)-α-Rha-(1→	100.2 <i>5.25</i>	78.1 <i>4.13</i>	71.4 <i>4.06</i>	82.3 <i>3.68</i>	70.8 <i>3.79</i>	18.5 <i>1.30</i>
497	→4)-β-Gal-(1→	105.6 <i>4.62</i>	73.5 <i>3.69</i>	75.0 <i>3.73</i>	79.2 <i>4.21</i>	76.3 <i>3.68</i>	63.0 <i>3.84; 3.79</i>
498							
499	β-Gal-(1→	105.6 <i>4.59</i>	73.4 <i>3.53</i>	74.2 <i>3.67</i>	70.5 <i>3.90</i>	76.8 <i>3.71</i>	62.6 <i>3.83; 3.78</i>
500	α-Ara-(1→	109.2 <i>5.11</i>	82.0 <i>4.09</i>	nd	nd	nd	nd

501

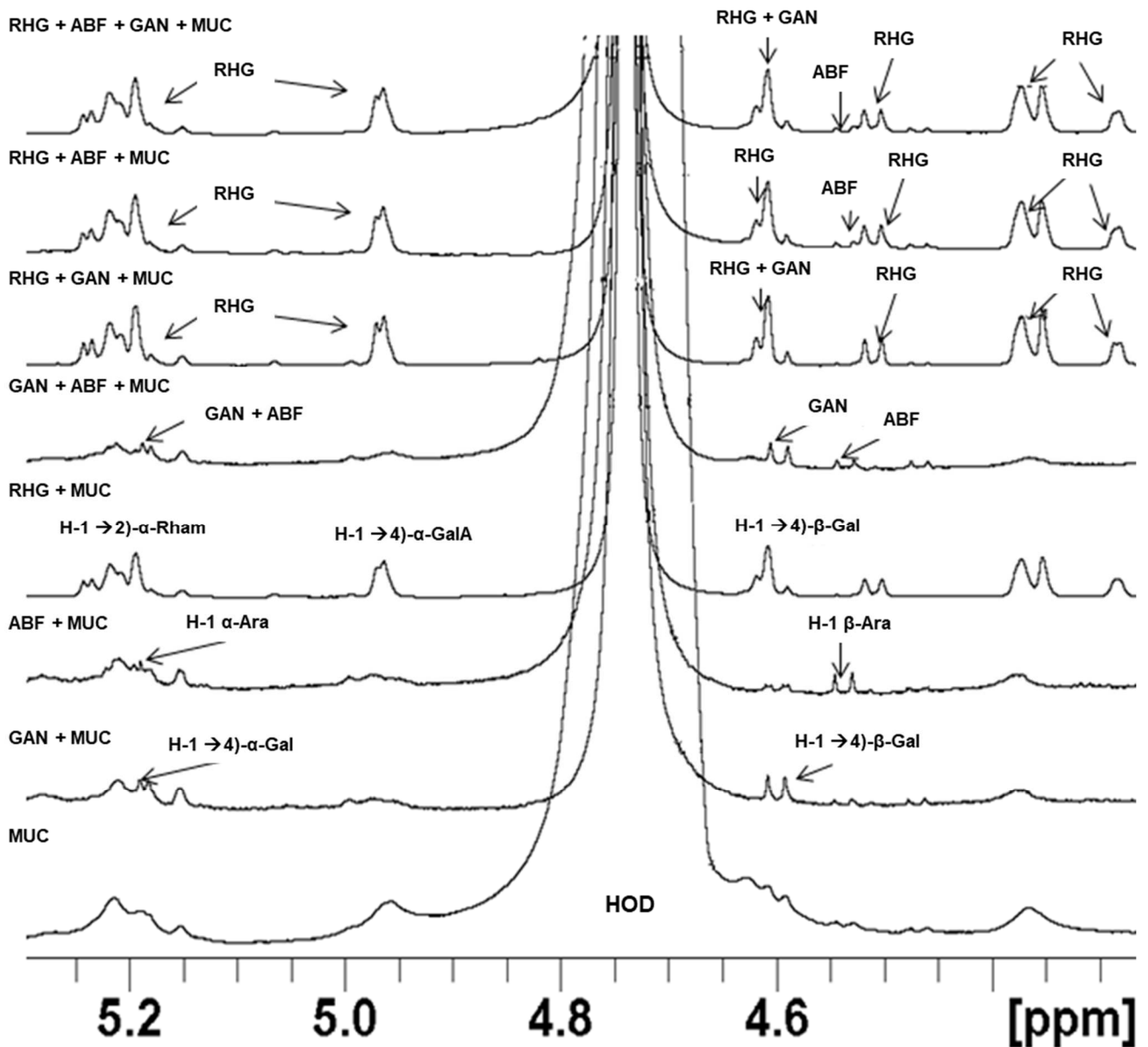
502 Considering this, it is noteworthy that camelina mucilage was different from flax seed  
 503 (Elboutachfaiti, et al 2017) or Arabidopsis thaliana seed mucilage (Yapo, 2011).

#### 504 ***Effects of RGlases on mucilage: from polysaccharide chemistry to viscosity***

505 In order to analyze the effects of RGlase on mucilage structure, and relate to  
 506 the above-mentioned results (**Fig. 4.A-D-G**) NMR analyses were carried out for all  
 507 recombinant enzymes independently or in combination (**Fig. 5**). As mentioned, the  
 508 relative activity on MUC was less than <10% for ABF, <1% for RHG, and null for  
 509 GAN (**Fig. 4A-D-G**). Due to the complexity and the viscosity of MUC, the three  
 510 enzymes were applied on this substrate in order to simplify its structure and to  
 511 determine the <sup>1</sup>H NMR spectrum (**Fig. 5**). The digestion of MUC by GAN showed  
 512 signals at 4.61 ppm (H-1 β-Gal) and 5.28 ppm (H-1 α-Gal) characteristic of galactose  
 513 linked in position 4. Thus, the 30% of galactose in MUC were mainly →4)-β-Gal-(1→,  
 514 and were the main side chains of MUC. The two signals at 5.24 ppm (α-Ara) and  
 515 4.51 ppm (β-Ara) in <sup>1</sup>H NMR spectrum (**Fig. 5**) inferred from ABF activity on MUC  
 516 were characteristic of arabinose monosaccharide. This arabinose represented 5 % of  
 517 the monosaccharide and was probably linked on galactose side chains. Spectrum of  
 518 the RHG activity on MUC (**Fig. 5**) showed signals deriving from a depolymerization of  
 519 the RGI backbone: →2)-α-Rha-(1→4)-α-GalA-(1→. The synergistic action of



520 enzymes on MUC was also tested. The main activity was observed for RHG with the  
 521 depolymerization of the backbone and minor action of the two other enzymes was  
 522 detected on sidechains. Despite their short size, the presence of side-chains of  
 523 arabino galactan and galactan could impact RGI polymer rheology. It was indeed  
 524 previously reported that the reduction of neutral sugar concentration can induce a  
 525 significant decrease in gelling temperature and viscosity (Sousa, Nielsen, Armagan,  
 526 Larsen & Sørensen, 2015).

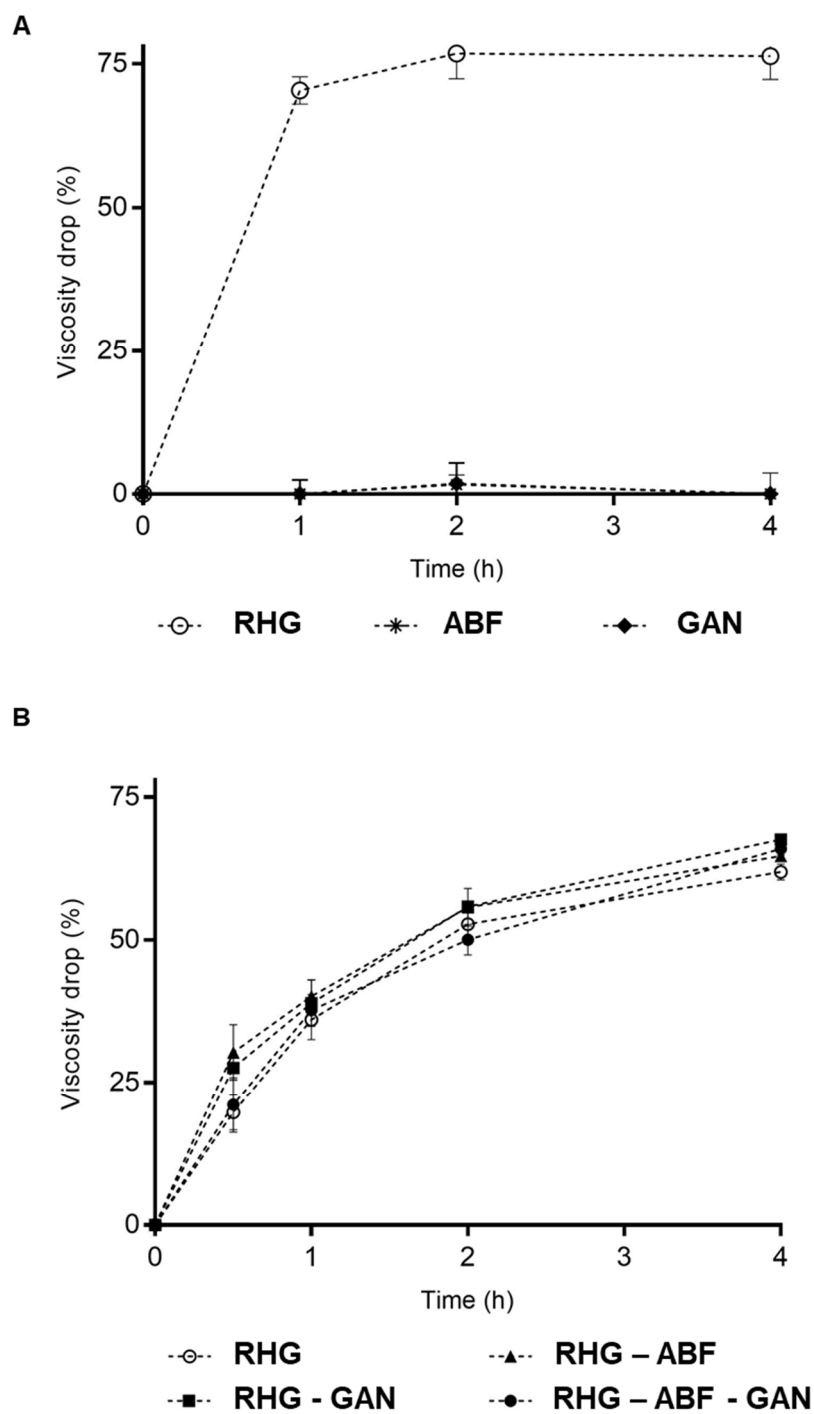


527  
 528 **Fig. 5.** <sup>1</sup>H proton NMR spectra of Camelina mucilage following treatment with RHG, ABF and GAN  
 529 recombinant enzymes. RHG: Endo-rhamnogalacturonase; ABF: α-Arabinofuranosidases; GAN: Endo-  
 530 β-1,4-galactanase.

531 To determine the applicative potential of characterized RGases, the  
532 changes in MUC viscosity were measured through a viscosity drop curve assay  
533 following application of the enzymes for 1 h to 4 h (**Fig. 6A-B**). The synergistic action  
534 of enzymes on MUC was studied by treating the substrate with each of the enzymes  
535 (RHG, ABF, and GAN) or binary-ternary mixtures (RHG-ABF, RHG-GAN, ABF-GAN,  
536 and RHG-ABF-GAN). *A. aculeatinus* RHG showed the highest efficiency in  
537 decreasing the viscosity on MUC compared to ABF and GAN, at a similar enzyme  
538 dose of 2  $\mu\text{g}$  (**Fig. 6A - Table S2**). The results revealed a significant drop (70 %) in  
539 viscosity as early as 1 h. Thus, to better discriminate the potential additive effects of  
540 the enzymes in mixture, 0.5  $\mu\text{g}$  of each enzyme was added and an early point of 30  
541 min was monitored. Binary and ternary mixtures lead to a further reduction in MUC  
542 viscosity as compared to RHG enzyme alone. Indeed, at 30 minutes RHG lowered  
543 the viscosity by 19 %, while RHG-GAN and RHG-ABF binary combinations led to a  
544 significant  $\sim 30$  % drop in viscosity (**Fig. 6B - Table S2**). In contrast, the effects of the  
545 RHG-ABF-GAN ternary combination was only a 21 % reduction in viscosity.  
546 At 4h, the highest viscosity drop was observed when using RHG-GAN and RHG-  
547 ABF-GAN combinations. A significant viscosity drop of 67.5 % was observed when  
548 using RHG-GAN mixture, compared to a 61.9 % viscosity drop generated by the  
549 single RHG enzyme (**Fig. 6B - Table S2**). As previously observed, the effect of the  
550 ternary combination on mucilage viscosity was less significant than that of binary  
551 mixtures. Therefore, it is likely that viscosity drop produced by RHG-GAN mixture  
552 was due to an additive effect of GAN, which potentially revealed cleavage sites for  
553 the RHG. This is consistent with the NMR analysis (**Fig. 5**), where RHG was shown  
554 to act on the RGI backbone (GalA  $\alpha$ -(1 $\rightarrow$ 2) Rha) while ABF-GAN were acting for the  
555 sidechains of arabinose (Ara  $\alpha$ -(1 $\rightarrow$ 3) Ara and Ara  $\alpha$ -(1 $\rightarrow$ 2) Ara) and galactose (Gal  
556  $\beta$ -(1 $\rightarrow$ 4) Gal).

557 Despite the statistical differences measured (**Table S2**), the viscosity was  
558 not drastically modified after 4 hours of treatment, probably related to the low  
559 contribution of GAN and ABF, considering the presence of short side-chains present  
560 in mucilage. Consistent with this results, HPSEC analyses (**Fig. S4**) revealed a shift  
561 in MW of the polymer after incubation with RHG enzyme, and a much lower effect  
562 mediated by ABF and GAN. Previous studies on apple pectins showed that the  
563 presence of RG-I side-chains allow pectin molecules to interact and entangle more,  
564 eventually creating a tighter conformation and decreasing molecular mobility (Hwang

565 & Kokini, 1992). However, the intrinsic viscosity is highly related to the number of  
566 side branches (Yapo, 2011). In our study, the RGI from *Camelina sativa* have a  
567 higher number of substitutions by galactose. Even so, the length of the branches  
568 appears to be insufficient to translate into long-term changes in viscosity following  
569 action of the accessory enzymes. It should also be noted that our results, by the  
570 chemical analysis of mucilage, provide a basis for identifying novel RGlases activities  
571 that can target short RGI side-chains. Probably, by increasing the dose of GAN  
572 enzyme or by having a two-step application (first GAN, second RHG), we could  
573 potentiate the changes in the viscosity of the polymer. Enzymatic treatment  
574 (pectinases) has been mostly used for plant seed mucilage to reduce viscosity before  
575 further processing (Wu, Li, Wang, Zhou & Mao., 2010). Hence, considering various  
576 doses and/or combinations of enzymes, a cocktail containing *A. aculeatinus* RGlases  
577 enzymes degrading sidechains and backbone, could be useful to improve the  
578 degradation process of RGI seed coat, allowing its use as structuring and texturizing  
579 agents for food or nutraceutical applications.



580

581 **Fig. 6.** Effects of RHG, ABF and GAN on mucilage viscosity over 4h incubation. (A) Single effect of  
 582 RHG, ABF, and GAN on the viscosity properties of camelina mucilage. (B) Synergism of RHG, ABF,  
 583 and GAN on the viscosity properties of camelina mucilage. RHG: Endo-rhamnogalacturonase; ABF:  $\alpha$ -  
 584 Arabinofuranosidases; GAN: Endo- $\beta$ -1,4-galactanase.

585

586

## 587 **CONCLUSION**

588           This study is the first full biochemical characterization of three RGI-degrading  
589 enzymes, a rhamnogalacturonase, a galactanase and an arabinofuranosidase, from  
590 *A. aculeatinus*. We were able to show that the three enzymes had an acidic pH  
591 optimum and that their optimal temperature for activity was 40-50°C. We assessed the  
592 substrate specificity of these three enzymes first on commercial substrates, showing  
593 that RHG acts on RGI as an endo enzyme, while ABF had a strong activity on arabinan  
594 with an exo mode of action. GAN was specific for →4)-β-Gal-(1→ linkages on galactan,  
595 with an endo mode of action. Using combined technical approaches, including NMR  
596 and viscosity assays, we were further able to relate the effects of the enzymes on a  
597 complex substrate, *Camelina sativa*'s mucilage, to potential industrial application. We  
598 first determined mucilage structure using 2D-NMR showing that it harbors short side-  
599 chains of galactose. We next showed that the use of binary combination of enzymes,  
600 led to a transient higher effect on mucilage viscosity, compared to the use of a single  
601 enzyme. This suggest that the short side galactose chains could explain the differential  
602 effects on mucilage's RGI-chemistry and viscosity. We believe that our study shed new  
603 light on the use, and the potential formulation, of these enzymes in industrial processes  
604 for which RGI hydrolysis is required. For instance, these novel enzymes could be used  
605 in fruit juice clarification, where RGI is known to be recalcitrant to digestion with  
606 commonly-used enzymatic cocktails.

607

## 608 **ACKNOWLEDGMENTS**

609 We wish to thank SAS-PIVERT for kindly providing the *Camelina sativa* seeds.

610

## 611 **FUNDING SOURCES**

612 This work was funded by a France Agrimer within the frame of the ENJOY (New  
613 Enzymes for Juice Optimal Yield) project (Programmes Agricoles et Agroalimentaires  
614 d'Avenir, 2017-0981) led by the Soufflet Group and in collaboration with the CTCPA.

615

## 616 **REFERENCES**

617 Adney, W. S., Jeoh, T., Beckham, G. T., Chou, Y. C., Baker, J. O., Michener, W.,  
618 Brunecky, R, & Himmel, M. E. (2009). Probing the role of N-linked glycans in

619 the stability and activity of fungal cellobiohydrolases by mutational analysis.  
620 *Cellulose*, 16(4), 699-709.

621 Arnous, A., & Meyer, A. S. (2009). Quantitative prediction of cell wall polysaccharide  
622 composition in grape (*Vitis vinifera* L.) and apple (*Malus domestica*) skins from  
623 acid hydrolysis monosaccharide profiles. *Journal of agricultural and food*  
624 *chemistry*, 57(9), 3611-3619.

625 Beldman, G., Searle-van Leeuwen, M. J. F., De Ruiter, G. A., Siliha, H. A., &  
626 Voragen, A. G. J. (1993). Degradation of arabinans by arabinanases from  
627 *Aspergillus aculeatus* and *Aspergillus niger*. *Carbohydrate Polymers*, 20(3),  
628 159–168.

629 Bertin, C., Pau-Roblot, C., Courtois, J., Manso-Silvan, L., Tardy, F., Poumarat, F.,  
630 Citti, C., Sirand-Pugnet, P., Gaurivaud, P., & Thiaucourt, F. (2015). Highly  
631 Dynamic Genomic Loci Drive the Synthesis of Two Types of Capsular or  
632 Secreted Polysaccharides within the *Mycoplasma mycoides* Cluster. *Applied*  
633 *and Environmental Microbiology*, 81(2), 676–687.

634 Bertin, C., Pau-Roblot, C., Courtois, J., Manso-Silvan, L., Thiaucourt, F., Tardy, F.,  
635 Grand, D. L., Poumarat, F., & Gaurivaud, P. (2013). Characterization of Free  
636 Exopolysaccharides Secreted by *Mycoplasma mycoides* Subsp. *mycoides*.  
637 *PLOS ONE*, 8(7), e68373.

638 Bretthauer, R. K., & Castellino, F. J. (1999). Glycosylation of *Pichia pastoris* -derived  
639 proteins. *Biotechnology and Applied Biochemistry*, 30(3), 193–200.

640 Chacon-Martınez, C. A., Anzola, J. M., Rojas, A., Hernandez, F., Junca, H., Ocampo,  
641 W., & Del Portillo, P. (2004). Identification and characterization of the  $\alpha$ -l-  
642 arabinofuranosidase B of *Fusarium oxysporum* f. sp. *dianthi*. *Physiological and*  
643 *Molecular Plant Pathology*, 64(4), 201–208.

644 Christgau, S., Sandal, T., Kofod, L. V., & Dalboge, H. (1995). Expression cloning,  
645 purification and characterization of a beta-1,4-galactanase from *Aspergillus*  
646 *aculeatus*. *Current Genetics*, 27(2), 135–141.

647 Crous, J. M., Pretorius, I. S., & van Zyl, W. H. (1996). Cloning and expression of the  
648  $\alpha$ -L-arabinofuranosidase gene (ABF2) of *Aspergillus niger* in *Saccharomyces*  
649 *cerevisiae*. *Applied Microbiology and Biotechnology*, 46(3), 256–260.

650 Cruz, A. K. M., Andrade, G. P. V., Chavante, S. F., de Vasconcelos, C. L., Garcia, R.  
651 B., Leite, E. L., Valente, A. P., Sales, M. P., & Oliveira, F. W. (2010). Structural

652 elucidation of an acidic galactan from the eggs of mollusc *Pomacea lineata*.  
653 *Carbohydrate Polymers*, 79(4), 975–980.

654 De Fine Licht, H. H., Schiøtt, M., Mueller, U. G., & Boomsma, J. J. (2010).  
655 Evolutionary transitions in enzyme activity of ant fungus gardens. *Evolution*,  
656 64, 2055-2069.

657 De Vries, R. P., Benen, J. A. E., de Graaff, L. H., & Visser, J. (2002). Plant Cell Wall  
658 Degrading Enzymes Produced by *Aspergillus*. In H. D. Osiewacz (Ed.),  
659 *Industrial Applications* (pp. 263–279). Springer.

660 De Vries, R. P., & Visser, J. (2001). *Aspergillus* enzymes involved in degradation of  
661 plant cell wall polysaccharides. *Microbiology and Molecular Biology Reviews* :  
662 *MMBR*, 65(4), 497–522.

663 De Wet, B. J. M., Matthew, M. K. A., Storbeck, K.-H., van Zyl, W. H., & Prior, B. A.  
664 (2008). Characterization of a family 54  $\alpha$ -l-arabinofuranosidase from  
665 *Aureobasidium pullulans*. *Applied Microbiology and Biotechnology*, 77(5),  
666 975–983.

667 Ding, H. H. Cui S.W., Goff H. D., Chen J., Wang Q., & Han N. F. (2015). Arabinan-  
668 rich rhamnogalacturonan-I from flaxseed kernel cell wall. *Food Hydrocolloids*  
669 47, 158–167.

670 Elboutachfai, R., Delattre, C., Quéro, A., Roulard, R., Duchêne, J., Mesnard, F., &  
671 Petit, E. (2017). Fractionation and structural characterization of six purified  
672 rhamnogalacturonans type I from flaxseed mucilage. *Food Hydrocolloids*, 62,  
673 273–279.

674 Flipphi, M. J. A., van Heuvel, M., van der Veen, P., Visser, J., & de Graaff, L. H.  
675 (1993). Cloning and characterization of the *abfB* gene coding for the major  $\alpha$ -l-  
676 arabinofuranosidase (ABF B) of *Aspergillus niger*. *Current Genetics*, 24(6),  
677 525–532.

678 González-Ayón, M. A., Licea-Claverie, Á., Valdez-Torres, J. B., Picos-Corrales, L. A.,  
679 Vélez-de la Rocha, R., Contreras-Esquivel, J. C., Labavitch, J. M., & Sañudo-  
680 Barajas, J. A. (2019). Enzyme-Catalyzed Production of Potato Galactan-  
681 Oligosaccharides and Its Optimization by Response Surface Methodology.  
682 *Materials (Basel, Switzerland)*, 12(9).

683 Grassin, C., & Fauquembergue, P. (1996). Wine and Fruit juices. *Industrial*  
684 *Enzymology*, 2. (Eds): T. Godfrey and S. West. Macmillan Press Ltd

685 Guo, Q., Cui, S. W., Wang, Q., & Young, J. C. (2008). Fractionation and  
686 physicochemical characterization of psyllium gum. *Carbohydrate Polymers*,  
687 *73*(1), 35-43.

688 Habrylo, O., Evangelista, D. E., Castilho, P. V., Pelloux, J., & Henrique-Silva, F.  
689 (2018). The pectinases from *Sphenophorus levis*: Potential for  
690 biotechnological applications. *International Journal of Biological*  
691 *Macromolecules*, *112*, 499–508.

692 Hwang, J., & Kokini, J. L. (1992). Contribution of the side branches to rheological  
693 properties of pectins. *Carbohydrate polymers*, *19*(1), 41-50.

694 Kashyap, D. R., Vohra, P. K., Chopra, S., & Tewari, R. (2001). Applications of  
695 pectinases in the commercial sector: a review. *Bioresource technology*, *77*(3),  
696 215-227.

697 Kofod, L. V., Kauppinen, S., Christgau, S., Andersen, L. N., Heldt-Hansen, H. P.,  
698 Dörreich, K., & Dalbøge, H. (1994). Cloning and characterization of two  
699 structurally and functionally divergent rhamnogalacturonases from *Aspergillus*  
700 *aculeatus*. *Journal of Biological Chemistry*, *269*(46), 29182–29189.

701 Koseki, T., Miwa, Y., Mese, Y., Miyanaga, A., Fushinobu, S., Wakagi, T., Shoun, H.,  
702 Matsuzawa, H., & Hashizume, K. (2006). Mutational analysis of N-glycosylation  
703 recognition sites on the biochemical properties of *Aspergillus kawachii*  $\alpha$ -L-  
704 arabinofuranosidase 54. *Biochimica et Biophysica Acta (BBA)-General*  
705 *Subjects*, *1760*(9), 1458-1464.

706 Le Nours, J., Ryttersgaard, C., Lo Leggio, L., Østergaard, P. R., Vedel Borchert, T.,  
707 Lehmann Hylling Christensen, L., & Larsen, S. (2003). Structures of two fungal  
708  $\beta$ -galactanases: Searching for the basis for temperature and pH optimum.  
709 *Protein Science*, *12*, 1195–1204.

710 Malik, M. R., Tang, J., Sharma, N., Burkitt, C., Ji, Y., Mykytyshyn, M., Bohmert-  
711 Tatarev, K., Peoples, O., & Snell, K. D. (2018). *Camelina sativa*, an oilseed at  
712 the nexus between model system and commercial crop. *Plant cell reports*,  
713 *37*(10), 1367-1381

714 McIlvaine, T. C. (1921). A buffer solution for colorimetric comparison. *Journal of*  
715 *Biological Chemistry*, *49*(1), 183–186.

716 Mikshina, P. V., Gurjanov, O. P., Mukhitova, F. K., Petrova, A. A., Shashkov, A. S., &  
717 Gorshkova, T. A. (2012). Structural details of pectic galactan from the



718 secondary cell walls of flax (*Linum usitatissimum* L.) phloem fibres.  
719 *Carbohydrate Polymers*, 87(1), 853–861.

720 Mikshina, P. V., Petrova, A. A., & Gorshkova, T. A. (2015a). Functional diversity of  
721 rhamnogalacturonans I. *Russian Chemical Bulletin*, 64(5), 1014-1023.

722 Mikshina, P. V., Idiyatullin, B. Z., Petrova, A. A., Shashkov, A. S., Zuev, Y. F., &  
723 Gorshkova, T. A. (2015b). Physicochemical properties of complex  
724 rhamnogalacturonan I from gelatinous cell walls of flax fibers. *Carbohydrate*  
725 *Polymers*, 117, 853–861.

726 Miller, G. L. (1959). Use of Dinitrosalicylic Acid Reagent for Determination of  
727 Reducing Sugar. *Analytical Chemistry*, 31(3), 426–428.

728 Mitchell, D. B., Vogel, K., Weimann, B. J., Pasamontes, L., & van Loon, A. P. G. M.  
729 (1997). The Phytase Subfamily of Histidine Acid Phosphatases: Isolation of  
730 Genes for Two Novel Phytases from the Fungi *Aspergillus Terreus* and  
731 *Myceliophthora Thermophila*. *Microbiology*, 143(1), 245–252.

732 Miyanaga, A., Koseki, T., Miwa, Y., Mese, Y., Nakamura, S., Kuno, A., Hirabayashi,  
733 J., Matsuzawa, H., Wakagi, T., Shoun, H., & Fushinobu, S. (2006). The family  
734 42 carbohydrate-binding module of family 54 alpha-L-arabinofuranosidase  
735 specifically binds the arabinofuranose side chain of hemicellulose. *The*  
736 *Biochemical Journal*, 399(3), 503–511.

737 Mohnen, D. (2008). Pectin structure and biosynthesis. *Current Opinion in Plant*  
738 *Biology*, 11(3), 266–277.

739 North, H. M., Berger, A., Saez-Aguayo, S., & Ralet, M.-C. (2014). Understanding  
740 polysaccharide production and properties using seed coat mutants: future  
741 perspectives for the exploitation of natural variants. *Annals of Botany*, 114(6),  
742 1251–1263.

743 Ollé, D., Baron, A., Lozano, Y. F., & Brillouet, J.-M. (2000). Enzymatic Degradation of  
744 Cell Wall Polysaccharides from Mango (*Mangifera indica* L.) Puree. *Journal of*  
745 *Agricultural and Food Chemistry*, 48(7), 2713–2716.

746 Pillon, M., Pau-Roblot, C., Lequart, V., Pilard, S., Courtois, B., Courtois, J., &  
747 Pawlicki-Jullian, N. (2010). Structural investigation of an exopolysaccharide  
748 substituted with a lactyl ether group produced by *Raoultella terrigena* Ez-555-6  
749 isolated in the Chernobyl exclusion zone. *Carbohydrate Research*, 345(9),  
750 1163–1173.

751 Rytioja, J., Hildén, K., Yuzon, J., Hatakka, A., de Vries, R. P., & Mäkelä, M. R.  
752 (2014). Plant-polysaccharide-degrading enzymes from Basidiomycetes.  
753 *Microbiology and Molecular Biology Reviews : MMBR*, 78(4), 614–649.

754 Ryttersgaard, C., Lo Leggio, L., Coutinho, P. M., Henrissat, B., & Larsen, S. (2002).  
755 *Aspergillus aculeatus* beta-1,4-galactanase: substrate recognition and  
756 relations to other glycoside hydrolases in clan GH-A. *Biochemistry*, 41(51),  
757 15135–15143.

758 Saha, B. C. (2000).  $\alpha$ -l-Arabinofuranosidases: biochemistry, molecular biology and  
759 application in biotechnology. *Biotechnology Advances*, 18(5), 403–423.

760 Sarv, V., Trass, O. and Diosady, L.L. (2017). Preparation and Characterization of  
761 *Camelina sativa* Protein Isolates and Mucilage. *Journal of the American Oil*  
762 *Chemists' Society*, 94: 1279-1285.

763 Shinozaki, A., Kawakami, T., Hosokawa, S., & Sakamoto, T. (2014). A novel GH43  $\alpha$ -  
764 l-arabinofuranosidase of *Penicillium chrysogenum* that preferentially degrades  
765 single-substituted arabinosyl side chains in arabinan. *Enzyme and Microbial*  
766 *Technology*, 58–59, 80–86.

767 Silva, I. R., Jers, C., Meyer, A. S., & Mikkelsen, J. D. (2016). Rhamnogalacturonan I  
768 modifying enzymes: an update. *New Biotechnology*, 33(1), 41–54.

769 Soukoulis, C., Gaiani, C., & Hoffmann, L. (2018). Plant seed mucilage as emerging  
770 biopolymer in food industry applications. *Current Opinion in Food Science*, 22,  
771 28–42.

772 Sousa, A. G., Nielsen, H. L., Armagan, I., Larsen, J., & Sørensen, S. O. (2015). The  
773 impact of rhamnogalacturonan-I side chain monosaccharides on the  
774 rheological properties of citrus pectin. *Food Hydrocolloids*, 47, 130-139.

775 Suykerbuyk, M. E., Kester, H. C., Schaap, P. J., Stam, H., Musters, W., & Visser, J.  
776 (1997). Cloning and characterization of two rhamnogalacturonan hydrolase  
777 genes from *Aspergillus niger*. *Applied and Environmental Microbiology*, 63(7),  
778 2507–2515.

779 Tapre, A., & Jain, R. (2014). Pectinases: Enzymes for fruit processing industry.  
780 *International Food Research Journal*, 21(2), 447-453.

781 Torpenholt, S., Poulsen, J. C. N., Muderspach, S. J., De Maria, L., & Lo Leggio, L.  
782 (2019). Structure of *Aspergillus aculeatus*  $\beta$ -1,4-galactanase in complex with  
783 galactobiose. *Acta Crystallographica. Section F, Structural Biology*  
784 *Communications*, 75(Pt 6), 399–404.

785 Ubeyitogullari, A., & Ciftci, O. N. (2020). Fabrication of bioaerogels from camelina  
786 seed mucilage for food applications. *Food Hydrocolloids*, *102*, 105597.

787 Van de Vis, J. W., Searle-van Leeuwen, M. J. F., Siliha, H. A., Kormelink, F. J. M., &  
788 Voragen, A. G. J. (1991). Purification and characterization of Endo-1,4- $\beta$ -D-  
789 galactanases from *Aspergillus niger* and *Aspergillus aculeatus*: Use in  
790 combination with arabinanases from *Aspergillus niger* in enzymic conversion  
791 of potato arabinogalactan. *Carbohydrate Polymers*, *16*(2), 167–187.

792 Vesth, T. C., Nybo, J. L., Theobald, S., Frisvad, J. C., Larsen, T. O., Nielsen, K. F.,  
793 Hoof, J. B., Brandl, J., Salamov, A., Riley, R., Gladden, J. M., Phatale, P.,  
794 Nielsen, M. T., Lyhne, E. K., Kogle, M. E., Strasser, K., McDonnell, E., Barry,  
795 K., Clum, A., Chen C., LaButti K., Haridas S., Nolan M., Sandor L., Kuo A.,  
796 Lipzen A., Hainaut M., Drula E., Tsang A., Magnuson J., Henrissat B.,  
797 Wiebenga A., Simmons B.A., Mäkelä M.R., de Vries R.P., Grigoriev I.V.,  
798 Mortensen U.H., Baker S.E., Andersen, M. R. (2018). Investigation of inter-  
799 and intraspecies variation through genome sequencing of *Aspergillus* section  
800 *Nigri*. *Nature Genetics*, *50*(12), 1688–1695.

801 Voragen, A. G. J., Coenen, G.-J., Verhoef, R. P., & Schols, H. A. (2009). Pectin, a  
802 versatile polysaccharide present in plant cell walls. *Structural Chemistry*,  
803 *20*(2), 263.

804 Voxeur, A., Habrylo, O., Guénin, S., Miart, F., Soulié, M.-C., Rihouey, C., Pau-Roblot,  
805 C., Domon, J.-M., Gutierrez, L., Pelloux, J., Mouille, G., Fagard, M., Höfte, H.,  
806 & Vernhettes, S. (2019). Oligogalacturonide production upon *Arabidopsis*  
807 *thaliana*–*Botrytis cinerea* interaction. *Proceedings of the National Academy of*  
808 *Sciences*, *116*(39), 19743–19752.

809 Wefers, D., Flörchinger, R., & Bunzel, M. (2018). Detailed structural characterization  
810 of arabinans and galactans of 14 apple cultivars before and after cold storage.  
811 *Frontiers in plant science*, *9*, 1451.

812 Wu, M., Li, D., Wang, L. J., Zhou, Y. G., & Mao, Z. H. (2010). Rheological property of  
813 extruded and enzyme treated flaxseed mucilage. *Carbohydrate Polymers*,  
814 *80*(2), 460-466.

815 Yapo, B. M. (2011). Rhamnogalacturonan-I: A Structurally Puzzling and Functionally  
816 Versatile Polysaccharide from Plant Cell Walls and Mucilages. *Polymer*  
817 *Reviews*, *51*(4), 391–413.

818 Zheng, Y., & Mort, A. (2008). Isolation and structural characterization of a novel  
819 oligosaccharide from the rhamnogalacturonan of *Gossypium hirsutum* L.  
820 *Carbohydrate Research*, 343(6), 1041–1049.  
821